

Grain refinement of magnesium alloys processed by severe plastic deformation

Yong-jun CHEN^{1,2,3}, Qu-dong WANG¹, Jin-bao LIN⁴, Man-ping LIU⁵, Jarle HJELEN², Hans J. ROVEN^{2,6}

1. National Engineering Research Center of Light Alloy Net Forming,
Shanghai Jiao Tong University, Shanghai 200030, China;

2. Department of Materials Science and Engineering, Norwegian University of Science and Technology,
Trondheim 7491, Norway;

3. ERC for Revolutionizing Metallic Biomaterials, North Carolina A&T State University,
Greensboro, NC 27411, USA;

4. School of Applied Science, Taiyuan University of Science and Technology, Taiyuan 030024, China;

5. School of Materials Science and Engineering, Jiangsu University, Zhenjiang 212013, China;

6. Center for Advanced Materials, Qatar University, Doha POB 2713, Qatar

Received 17 October 2013; accepted 22 November 2014

Abstract: Grain refinement of AZ31 Mg alloy during cyclic extrusion compression (CEC) at 225–400 °C was investigated quantitatively by electron backscattering diffraction (EBSD). Results show that an ultrafine grained microstructure of AZ31 alloy is obtained only after 3 passes of CEC at 225 °C. The mean misorientation and the fraction of high angle grain boundaries (HAGBs) increase gradually by lowering extrusion temperature. Only a small fraction of $\{10\bar{1}2\}$ twinning is observed by EBSD in AZ31 Mg alloys after 3 passes of CEC. Schmid factors calculation shows that the most active slip system is pyramidal slip $\{10\bar{1}1\}$ $(11\bar{2}0)$ and basal slip $\{0001\}$ $(11\bar{2}0)$ at 225–350 °C and 400 °C, respectively. Direct evidences at subgrain boundaries support the occurrence of continuous dynamic recrystallization (CDRX) mechanism in grain refinement of AZ31 Mg alloy processed by CEC.

Key words: magnesium alloys; grain refinement; continuous dynamic recrystallization (CDRX); electron backscattering diffraction (EBSD); cyclic extrusion compression (CEC)

1 Introduction

Magnesium alloys are the lightest metal structural materials and are much lighter than aluminum alloys and steel [1,2]. They are used in various applications which include national defense, automobiles, etc, due to their low density, high specific strength and excellent machinability [3,4]. There are increasingly strict demands for Mg alloys at both strength and ductility, especially for the activation of big projects including lunar excursion, high speed traffic tools and electronic automobiles. However, most Mg alloys generally present limited ductility and strength at ambient temperature, which severely limits their industrial application.

Grain refinement by severe plastic deformation (SPD) is a well-known method to improve both strength and ductility of metals [5]. According to the Hall–Petch relationship and Taylor factor, the yield strength of metals is associated with not only grain size but also number of slip systems. Therefore, the contribution of grain refinement on the strength of Mg alloys is much greater than the other metals with more slip systems, e.g., face-centered cubic (FCC) and body-centered cubic (BCC) metals [6]. Among all available SPD methods [7], cyclic extrusion compression (CEC) is very suitable for grain refinement of Mg alloys due to its characteristics of continuous deformation and special stress condition. The CEC method was designed originally for fabricating pure Al and its alloys [8,9]. Our group has extended its

Foundation item: Projects (50674067, 51074106, 51374145) supported by the National Natural Science Foundation of China; Project (09JC1408200) supported by the Science and Technology Commission of Shanghai Municipality, China; Project (2011BAE22B01-5) supported by the National Key Technology R & D Program of China; Projects (182000/S10, 192450/I30) supported by the Research Council of Norway

Corresponding authors: Qu-dong WANG; Tel: +86-21-54742715; E-mail: wangqudong@sjtu.edu.cn; Hans J. Roven; Tel: +47-73594966; E-mail: hans.roven@material.ntnu.no

DOI: 10.1016/S1003-6326(14)63528-7

application to Mg alloys [10–12]. In our recent works, we have studied the microstructure evolution of AZ31 Mg alloy after CEC 1–7 passes [10], the effect of the second phase on the microstructure evolution of AZ series Mg alloys [11], and a proposed compound grain refinement mechanism including rotational dynamic recrystallization (RDRX) and continuous dynamic recrystallization (CDRX) [12]. However, we have not presented any solid evidence for the suggested CDRX of Mg alloys processed by CEC. Moreover, the effect of extrusion temperature on the grain refinement of Mg alloys is still unknown.

This present work aims to bring more insight in the grain refinement of AZ31 Mg alloy during CEC at 225–400 °C and provide solid evidence for the suggested CDRX.

2 Experimental

AZ31 Mg alloy (Mg–3.09%Al–1.02%Zn–0.42%Mn, mass fraction) extruded bar and the die were firstly held at 100 °C for 10 min, and were coated with graphite as lubricant. Then, they were kept at targeting temperature for about 2 h. The samples were put into the upper chamber to start the CEC processing cycle. The operation of CEC was detailed in Refs. [9,10]. All samples were quenched in water immediately after CEC deformation to keep the deformed microstructure. Longitudinal section of CEC bar was prepared for optical microscopy, TEM and EBSD observations. Details of the sample preparations for EBSD and TEM can be found in Ref. [11].

3 Results and discussion

3.1 Grain refinement by increasing strain

In our previous report [10], grain refinement of AZ31 Mg alloy processed by CEC 1–7 passes at 300 °C was studied. Figures 1(a) and (b) illustrate the copies of initial and processed microstructures. It can be seen that a typical heterogeneous microstructure of the as-extruded AZ31 Mg alloy is shown in Fig. 1(a). After CEC 7 passes, the microstructure is reasonably homogeneous and the grains are equiaxed. A mean grain size of 1.77 μm is obtained [10]. With further deformation up to 15 passes, the grain size is slightly reduced but a coarse-grain region is clearly shown in Fig. 1(c). This indicates that the microstructure reaches a dynamic balance between grain refinement by strain and grain growth by high temperature during CEC processing. Hence, it can be concluded that there exists a critical CEC pass to obtain a balance microstructure under a given temperature. This result is in accordance with the effect of extrusion ratio on the microstructure and mechanical properties of AZ31 Mg alloy [13].

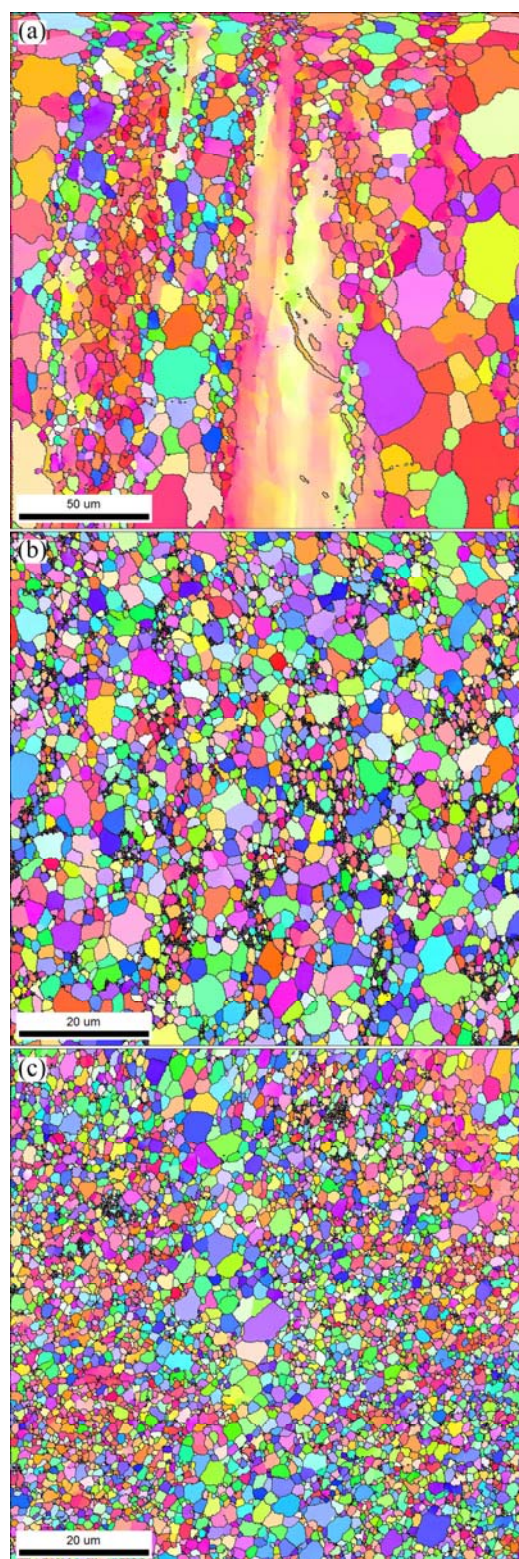


Fig. 1 Orientation maps of AZ31 Mg alloy after CEC at 300 °C: (a) As-extruded; (b) 7 passes; (c) 15 passes

3.2 Grain refinement by lowering extrusion temperature

Figure 2 shows the orientation maps of AZ31 alloy processed by 3 passes of CEC at 225–400 °C. The

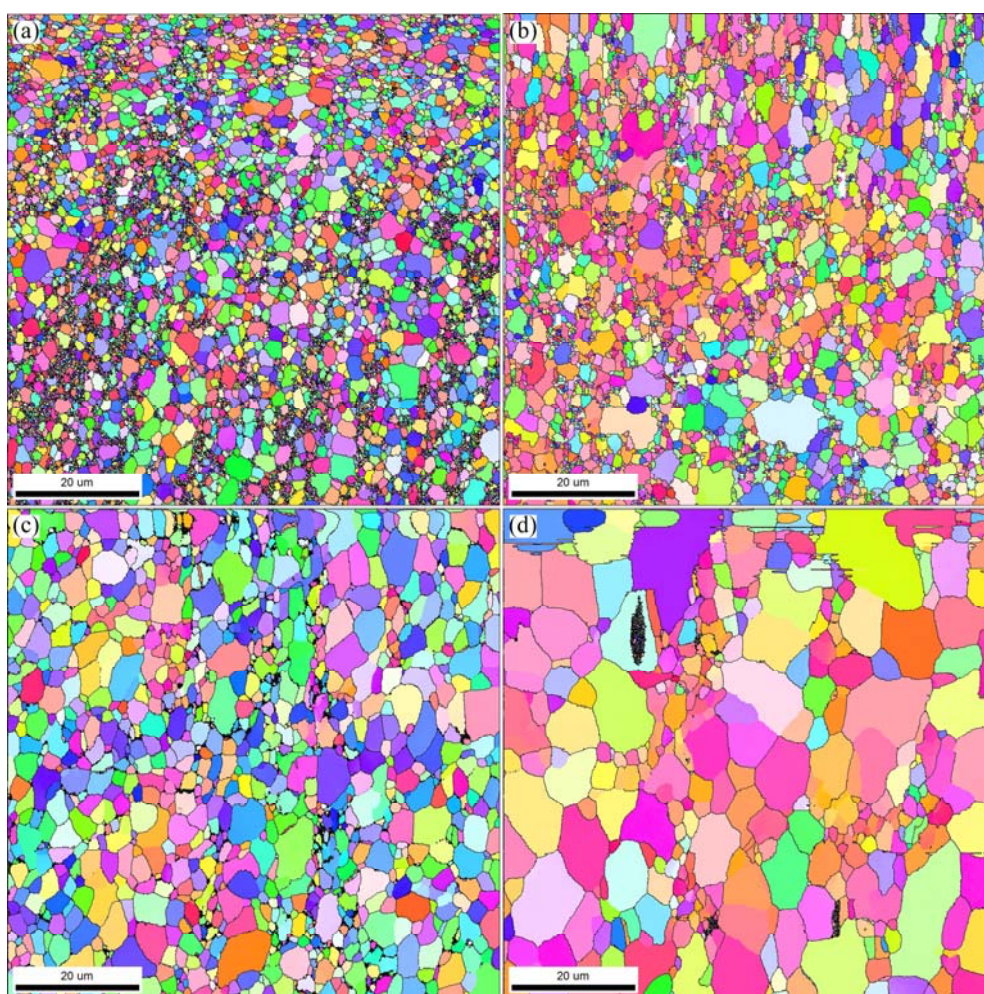


Fig. 2 Orientation maps of AZ31 Mg alloy processed by 3 passes of CEC at different temperatures: (a) 225 °C; (b) 300 °C; (c) 350 °C; (d) 400 °C

microstructure is refined gradually by decreasing extrusion temperature. It is interesting to note that the fine grains in Figs. 2(a) and (b) tend to form network-shaped structures [12]. It should be noted that some of the fine grains in the network-shaped structures may have non-indexed pixels (confidence index (CI) < 0.08) because of the poor quality of the Kikuchi patterns associated with heavy deformation. The grain size distributions of Fig. 2 are shown in Fig. 3 (The pixels with CI < 0.08 have been removed). It can be seen that the distribution range of grain size decreases continuously by lowering temperature from 400 to 225 °C. The fraction of HAGBs and the mean grain size, and the mean misorientation are summarized as a function of extrusion temperature in Fig. 4 and Table 1, respectively. The fractions of HAGBs and the mean misorientation increase continuously as temperature decreases, which indicates that lowering the temperature promotes the evolution of LAGBs into HAGBs. This result agrees with the fact that the mean grain size of processed microstructures decreases with decreasing extrusion

temperature, as shown in Fig. 4. The mean grain size of AZ31 Mg alloy after 3 passes of CEC at 225 °C is 0.62 μm, which is smaller than the mean grain size of 1.77 μm of 7 passes of CEC at 300 °C. It is therefore important to optimize the strain and extrusion temperature. The reason to have this great effect on grain size is that the thermally activated processes of recovery and grain growth can be greatly suppressed by lowering the extrusion temperature.

Kernel average misorientation (KAM) shows the distribution of local misorientation based on a Kernel average misorientation between neighbors on the scan grid [14]. It is an important indicator of dislocation density [15] and strain distribution on individual measurement points [16]. Figure 5 shows the calculated distribution of processed AZ31 alloy with the provision that misorientations exceeding 15° (HAGBs) are excluded. In this calculation, only the first neighbor in the kernel has been considered. It can be observed that the KAM peaks tend to move towards the left side with increasing extrusion temperature (see Fig. 5), which

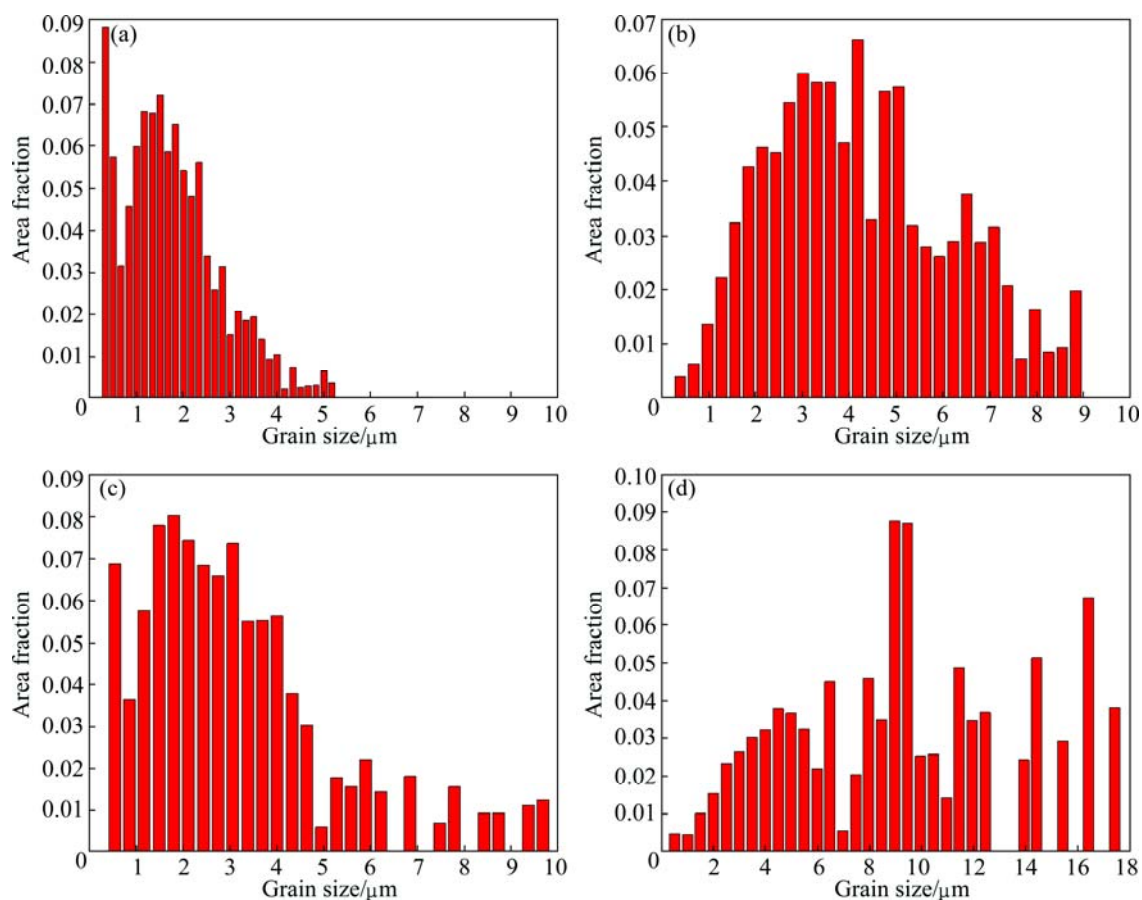


Fig. 3 Grain size distributions of AZ31 Mg alloy processed by 3 passes of CEC at different temperatures: (a) 225 °C; (b) 300 °C; (c) 350 °C; (d) 400 °C

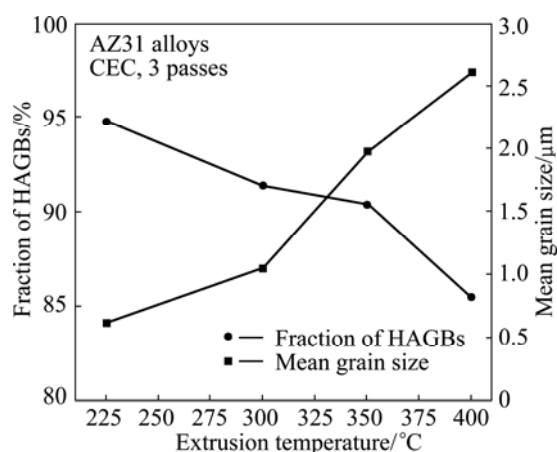


Fig. 4 Fraction of HAGBs and mean grain size as function of extrusion temperature

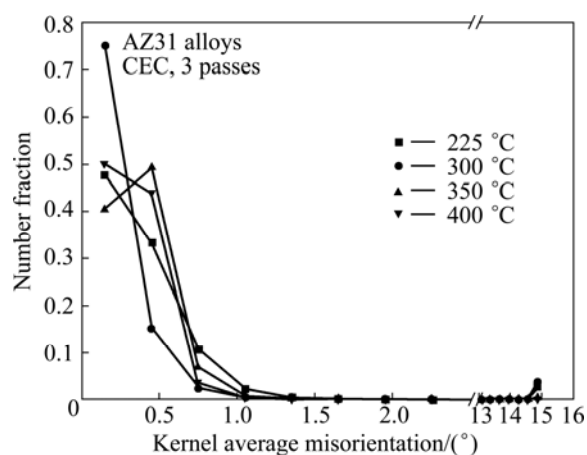


Fig. 5 Kernel average misorientation distribution of AZ31 Mg alloy processed by 3 passes of CEC

Table 1 Summary of mean misorientation and Kernel average misorientation of AZ31 alloy processed by CEC

CEC temperature/°C	Mean misorientation/(°)	Kernel average misorientation/(°)
225	51	0.84
300	48.9	0.83
350	47.3	0.49
400	42.5	0.39

results in the fact that the mean value of KAM decreases from 0.84 at 225 °C to 0.39 at 400 °C (see Table 1). The evolution of KAM with extrusion temperature indicates that strain and dislocation density increase by simply lowering extrusion temperature.

In our previous study, $\{10\bar{1}2\}$ twinning has been observed by TEM in AZ31 Mg alloy processed by CEC at 300 °C [12]. EBSD can investigate a much bigger area

and it is therefore possible to provide a full overview of the twins. Figure 6 shows an example of $\{10\bar{1}2\}$ twinning confirmed by the EBSD technique, which is activated in AZ31 Mg alloy during 3 passes of CEC at 350 °C. A twin and the matrix are highlighted in red and blue, respectively, which meet two criteria suggested by MASON et al [17] and NAVE et al [18] for a coherent twinning. Firstly, the highlighted grains (red is marked by circle and blue is marked by square in the pole figures) on either side of the boundary have coincident $\{10\bar{1}2\}$ plane normals, as can be seen in the overlapping of the circle and square in the $\{10\bar{1}2\}$ pole figure in Fig. 6(c). Secondly, these plane normals are coincident with the boundary trace normal, seen as the parallel green dashed lines in Figs. 6(a) and (c). The occurrence of $\{10\bar{1}2\}$ twinning shows that a small fraction of coarse grains with unfavorable orientation for slip systems are still observed in the large strained AZ31 Mg alloys after 3 passes of CEC, even though dislocation slip is obviously dominant. It is important to point out that no other primary or secondary twinning modes are detectable in the present work. The fraction of twins in Figs. 2(a)–(d) is generally less than 4.4% and no obvious tendency can be obtained as a function of extrusion temperature. This is probably due to the competition of grain size and extrusion temperature. Taking Fig. 2(a) for example, the lowest extrusion temperature favors the formation of twins and ultrafine grains by suppressing grain growth. However, the formation of ultrafine grains does not favor the further formation of twins because of the grain size effect.

In general, Schmid factor is one of the most important factors affecting the deformation mechanism and the operation of slip systems in Mg alloys [19]. Schmid's law can be written as

$$\tau_{cr} = \sigma \cos \phi \cos \lambda = \sigma M$$

where τ_{cr} is the critical resolved shear stress (CRSS) of a given slip system, which is known to vary significantly among various slip systems in hexagonal close-packed (HCP) crystals [19]; σ is the applied stress; ϕ and λ are the angles between the extrusion axis and the slip plane normal and the shear direction, respectively; M is the Schmid factor.

Figure 7 shows the Schmid factor distributions of AZ31 Mg alloy processed by 3 passes of CEC at 225–400 °C. Four possible slip systems have been calculated, including basal slip $\{0001\}\langle 11\bar{2}0\rangle$, prismatic slip $\{10\bar{1}0\}\langle 11\bar{2}0\rangle$ and pyramidal slips $\{10\bar{1}1\}\langle 11\bar{2}0\rangle$ and $\{11\bar{2}2\}\langle 11\bar{2}3\rangle$. It can be seen that all slip systems listed above seem to be activated during 3 passes of CEC at 225–400 °C. It is apparent that $\{10\bar{1}1\}\langle 11\bar{2}0\rangle$ at temperature of 225–350 °C (Figs. 7(a)–(c)) and $\{0001\}\langle 11\bar{2}0\rangle$ at 400 °C (Fig. 7(d)) show a high frequency of high Schmid factors, which indicates that the most active slip system is pyramidal slips $\{10\bar{1}1\}\langle 11\bar{2}0\rangle$ during 225–350 °C and basal slip $\{0001\}\langle 11\bar{2}0\rangle$ at 400 °C. This result agrees with the orientation maps in Fig. 2 that $\{0001\}$ orientation (red color) is dominant in Fig. 2(d). It is reported that basal slip is dominant in magnesium when deformation is at room temperature and the tendency of non-basal slip increases with increasing temperature. The CRSS for basal and non-basal slips is almost the same order at temperatures above 327 °C [20]. In addition, the mean grain sizes of AZ31 Mg alloy after 3 passes of CEC are very small, which indicates much better deformation ability and changed deformation mechanism compared with the conventional coarse grained AZ31 alloy.

3.3 Grain refinement mechanism during CEC

As mentioned above, CEC deformation is a cyclic combination of extrusion and compression, which results

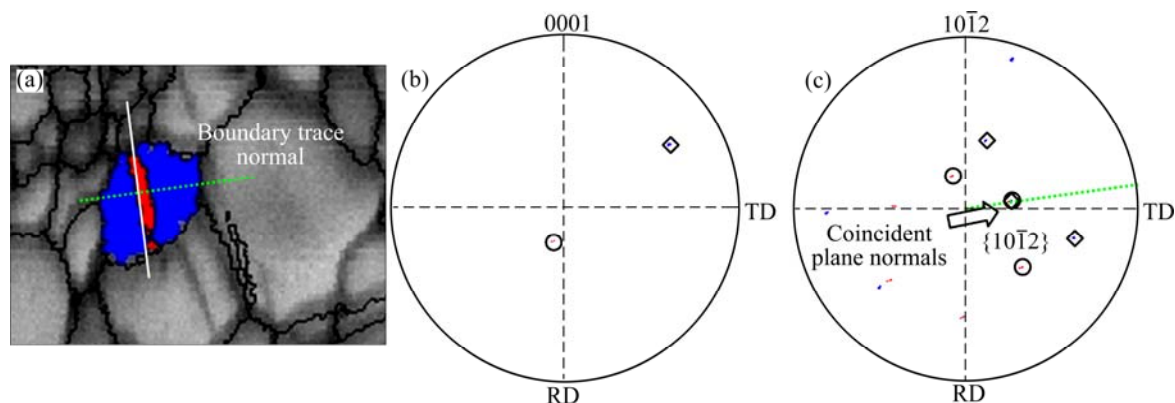


Fig. 6 EBSD conformation of $\{10\bar{1}2\}$ twins in microstructure of AZ31 Mg alloy processed by 3 passes of CEC at 350 °C: (a) Grain boundary map showing $\{10\bar{1}2\}$ twin boundaries (87.4°) with twin and matrix highlighted by red and blue, respectively; (b) Corresponding $\{0001\}$ pole figure showing rotation of twin away from matrix; (c) $\{10\bar{1}2\}$ pole figure showing twin interior orientation sharing common pole with matrix, with green dashed line parallel to boundary trace normal (Fig. 6(a))

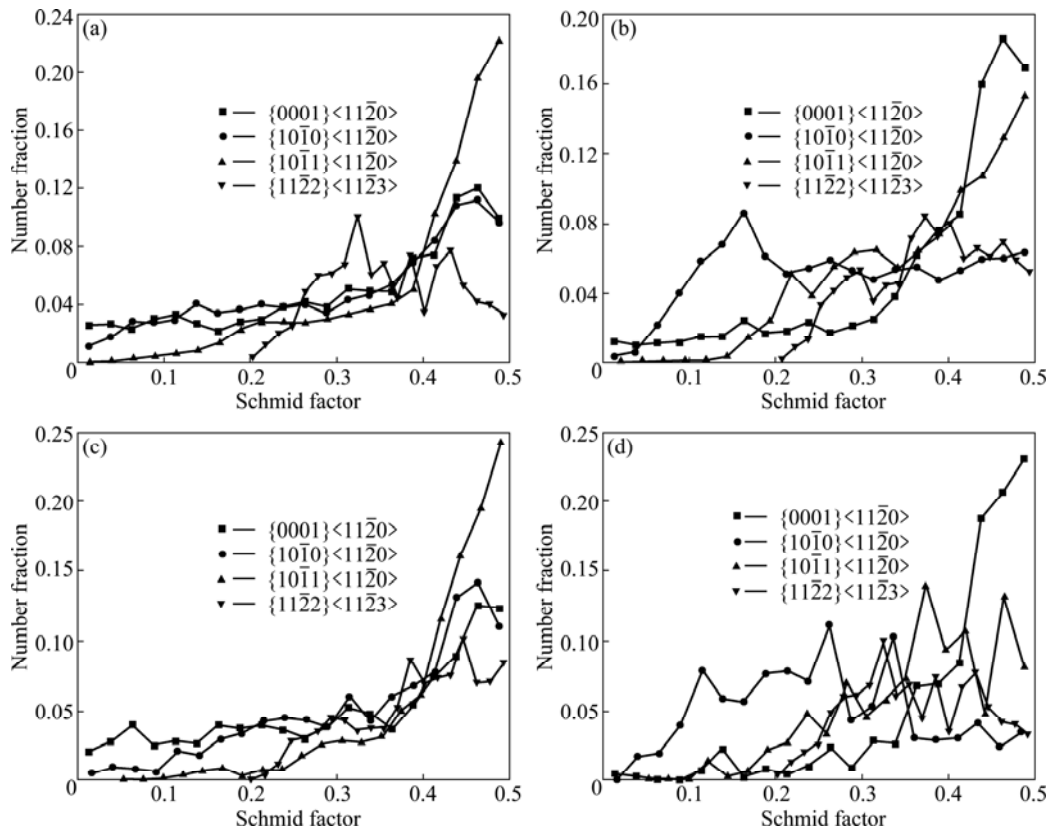


Fig. 7 Schmid factor distributions of AZ31 Mg alloy processed by passes of CEC 3 at 225 °C (a), 300 °C (b), 350 °C (c) and 400 °C (d)

in a lot of dislocations in the microstructure, as shown in Fig. 8. High density dislocations are observed inside some coarse grains (see Fig. 8(a)) and tangle each other to form dislocation networks (see Fig. 8(b)). In order to decrease system distortion energy, dislocations will rearrange by spontaneous interaction when the dislocation density is high enough inside grains [21]. Figure 8(c) shows that a typical subgrain boundary has been formed by dislocations rearrangement. These subgrain boundaries with loose zones confirm that they are formed by the rearrangement of dislocation networks.

Figure 9(a) shows the typical subgrain boundaries in Mg alloy after CEC. The grain boundaries with clear and smooth line are HAGBs. The subgrain boundaries, formed by dislocation rearrangement inside grains with HAGBs, have low misorientation and tend to evolve into HAGBs through merging or absorbing of lattice dislocations. Figure 9(b) reveals that the subgrain boundaries are absorbing the dislocations from either side of the subgrain boundaries. The subgrain boundaries will evolve into stable HAGBs and the coarse grains are therefore refined through CDRX. The present observation of dislocation networks evolving into subgrain boundaries is in good agreement with the model suggested by VALIEV et al [21].

There are several details in the magnified orientation maps that provide solid evidence to support the occurrence of CDRX in AZ31 Mg alloy during CEC

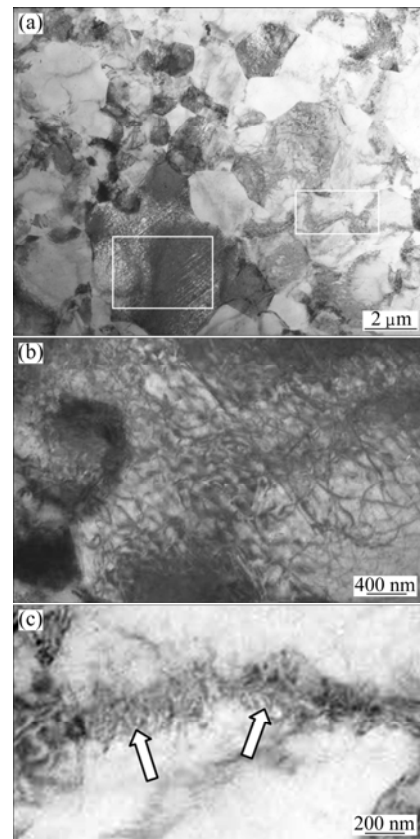


Fig. 8 High density dislocations in some coarse grains (a), dislocation networks (b) and rearrangement subgrain boundaries (c) in AZ31 Mg alloy after 3 passes of CEC at 300 °C

processing. As can be seen in Fig. 10(a), the unit cells rotate slightly in a certain manner from the coarse grains to the new formed fine grains. This gradual lattice rotation induced by strain is believed to be CDRX. Moreover, LAGBs segments (white lines, examples marked by arrows *A* in Figs. 10(a) and (b)) can be frequently found inside relatively coarse grains, which agree with the continuous formation of LAGBs by absorbing dislocations (Figs. 8 and 9). More careful investigation shows that new HAGBs are formed by the progressive evolution of LAGBs, which can be revealed from the fact that incomplete HAGBs are connected by LAGBs (an example is marked by arrow *B* in Fig. 10(a)).

4 Conclusions

1) An ultrafine grained microstructure of AZ31

alloy is obtained only after 3 passes of CEC at 225 °C.

2) Grain refinement of AZ31 Mg alloy is obviously affected by the extrusion temperature. The mean misorientation and the fraction of high angle grain boundaries increase gradually by lowering the extrusion temperature.

3) Only $\{10\bar{1}2\}$ twinning is detected in AZ31 Mg alloy during 3 passes of CEC.

4) Dislocation slip is dominant in AZ31 Mg alloy during 3 passes of CEC. Schmid factors calculation shows that the most active slip system is pyramidal slip $\{10\bar{1}1\}\langle 11\bar{2}0\rangle$ and basal slip $\{0001\}\langle 11\bar{2}0\rangle$ at 225–350 °C and 400 °C, respectively.

5) Analysis on subgrain boundaries by both TEM and EBSD provides solid evidence on the occurrence of CDRX mechanism in grain refinement of AZ31 Mg alloys during CEC.

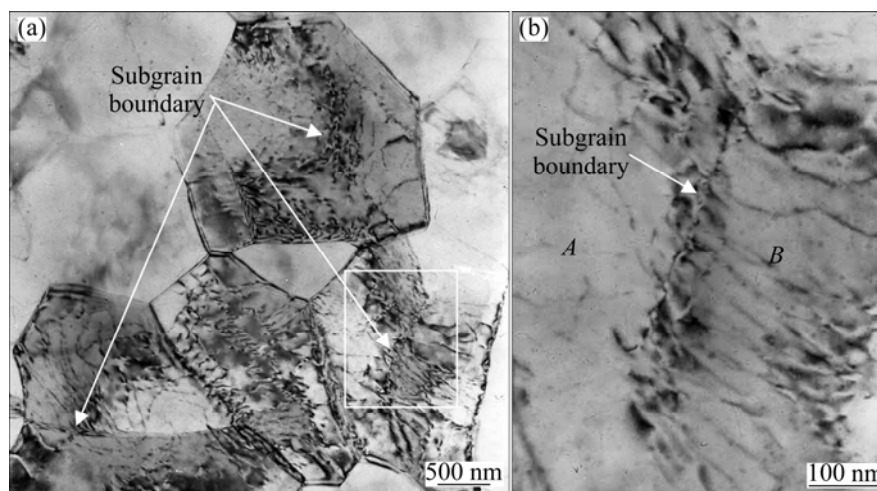


Fig. 9 Subgrains in AZ31 Mg alloy during 3 passes of CEC at 250 °C (a) and subgrain boundary showing absorption of dislocations (b)

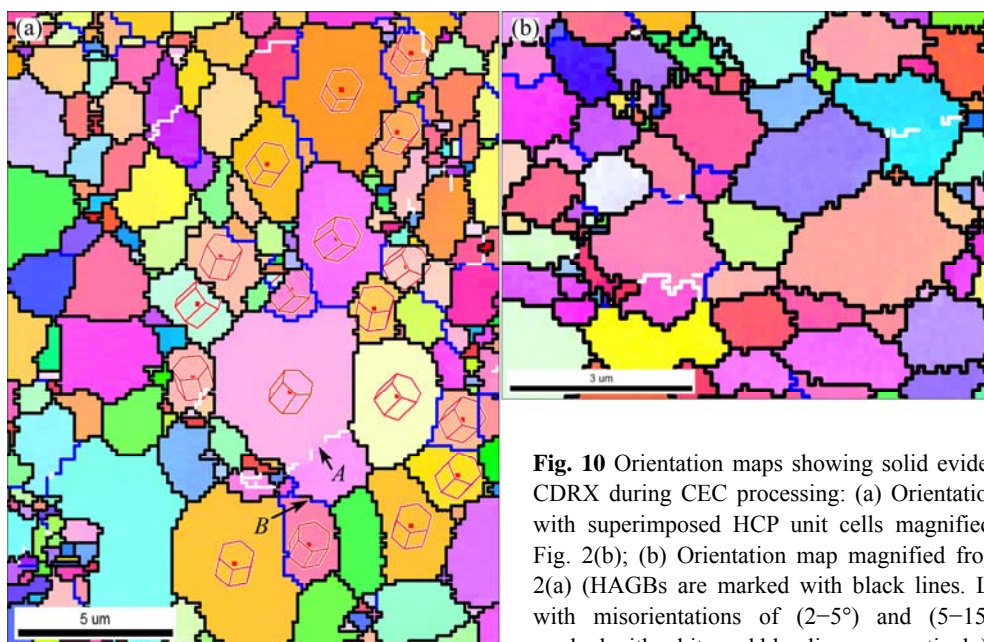


Fig. 10 Orientation maps showing solid evidence of CDRX during CEC processing: (a) Orientation map with superimposed HCP unit cells magnified from Fig. 2(b); (b) Orientation map magnified from Fig. 2(a) (HAGBs are marked with black lines. LAGBs with misorientations of (2–5°) and (5–15°) are marked with white and blue lines, respectively)

References

- [1] CHEN Yong-jun, WANG Qu-dong, ZHAI Chun-quan, DING Wen-jiang. Research and development prospects of high strength Mg alloys fabricated by severe plastic deformation [J]. Mater Mech Eng, 2006, 30(3): 1–3 (in Chinese)
- [2] DECKER R F. The renaissance in magnesium [J]. Advanced Mater & Proc, 1998(9): 31–35.
- [3] FROES F H, ELIEZER D, AGHION E. The science, technology and applications of magnesium [J]. JOM, 1998(9): 30–33.
- [4] WANG Qu-dong, DING Wen-jiang. The recent advances of magnesium alloys and their forming techniques [C]//Materials Processing Technique and Science in 21st Century. Beijing: Mechanical Industry Press, 2004: 56–73.
- [5] VALIEV R Z, ISLAMGALIEV P K, ALEXANDROV I V. Bulk nanostructured materials from severe plastic deformation [J]. Prog Mater Sci, 2000, 45(2): 103–189.
- [6] VALIEV R Z, ZEHETBAUER M J, ESTRIN Y, HOPPEL H W, IVANISENKO Y L, HAHN H, GERHARD W, ROVEN H J, SAUVAGE X, LANGDON T G. The innovation potential of bulk nanostructured materials [J]. Adv Eng Mater, 2007, 9(7): 527–533.
- [7] AZUSHIMA A, KOPP R, KORHONEN A, YANG D Y, MICARI F, LAHOTI G D, GROCHE P, YANAGIMOTO J, TSUJI N, ROSOCHOWSKI A, YANAGIDA A. Severe plastic deformation (SPD) processes for metals [J]. CIRP annals Manuf Technol, 2008, 57(2): 716–735.
- [8] YEH J W, YUAN S Y, PENG C H. A reciprocating extrusion process for producing hypereutectic Al–20wt.% Si wrought alloys [J]. Mater Sci Eng A, 1998, 252(2): 212–221.
- [9] RICHERT M, LIU Q, HANSEN N. Microstructural evolution over a large strain range in aluminium deformed by cyclic-extrusion-compression [J]. Mater Sci Eng A, 1999, 260(1–2): 275–283.
- [10] CHEN Y J, WANG Q D, ROVEN H J, KARLSEN M, YU Y D, LIU M P, HJELEN J. Microstructure evolution in magnesium alloy AZ31 during cyclic extrusion compression [J]. J Alloys Compd, 2008, 462(1–2): 192–200.
- [11] WANG Q D, CHEN Y J, LIU M P, LIN J B, ROVEN H J. Microstructure evolution of AZ series magnesium alloys during cyclic extrusion compression [J]. Mater Sci Eng A, 2010, 527(9): 2265–2273.
- [12] CHEN Y J, WANG Q D, ROVEN H J, LIU M P, KARLSEN M, YU Y D, HJELEN J. Network-shaped fine-grained microstructure and high ductility of magnesium alloy fabricated by cyclic extrusion compression [J]. Scripta Mater, 2008, 58(4): 311–314.
- [13] CHEN Y J, WANG Q D, PENG J G, ZHAI C Q, DING W J. Effects of extrusion ratio on the microstructure and mechanical properties of AZ31 Mg alloy [J]. J Mater Process Technol, 2007, 182(1–3): 281–285.
- [14] EDAX. OIM analysis 5.3 software user manual [M]. UT, USA: EDAX/TSI, 2007.
- [15] LI H, HSU E, SZPUNAR J, UTSUNOMIYA H, SAKAI T. Deformation mechanism and texture and microstructure evolution during high-speed rolling of AZ31B Mg sheets [J]. J Mater Sci, 2008, 43: 7148–7156.
- [16] WRIGHT S I, NOWELL M M, FIELD D P. A review of strain analysis using electron backscatter diffraction [J]. Microsc Microanal, 2011, 17: 316–329.
- [17] MASON T A, BINGERT J F, KASCHNER G C, WRIGHT S I, LARSEN R J. Advances in deformation twin characterization using electron backscattered diffraction data [J]. Metall Mater Trans A, 2002, 33(13): 949–954.
- [18] NAVE M D, MULDER J J L, GHOLINIA A. Twin characterization using 2D and 3D EBSD [J]. Chin J Stereo Image Anal, 2005, 10(4): 199–204.
- [19] SMALLMAN R E, BISHOP R J. Metals and materials: Science, process, applications [M]. London: Butterworth-Heinemann (Oxford and Boston), 1995: 206.
- [20] LIU Y, WU X. An electron-backscattered diffraction study of the texture evolution in a coarse-grained AZ31 magnesium alloy deformed in tension at elevated temperatures [J]. Metall Mater, 2006, 37A: 7–17.
- [21] VALIEV R Z, IVANISENKO Y V, RAUCH E F, BAUDELET B. Structure and deformation behavior of Armco iron subjected to severe plastic deformation [J]. Acta Mater, 1996, 44(12): 4705–4712.

大塑性变形镁合金的晶粒细化

陈勇军^{1,2,3}, 王渠东¹, 林金保⁴, 刘满平⁵, Jarle HJELEN², Hans J. ROVEN^{2,6}

1. 上海交通大学 轻合金精密成型国家工程研究中心, 上海 200030;

2. Department of Materials Science and Engineering, Norwegian University of Science and Technology, Trondheim 7491, Norway;

3. ERC for Revolutionizing Metallic Biomaterials, North Carolina A&T State University, Greensboro, NC 27411, USA;

4. 太原科技大学 应用科学学院, 太原 030024;

5. 江苏大学 材料科学与工程学院, 镇江 212013;

6. Center for Advanced Materials, Qatar University, POB 2713 Doha, Qatar

摘要: 采用电子背散射技术(EBSD)定量研究 AZ31 镁合金在 225~400 °C 往复挤压大变形过程中的晶粒细化。结果表明: 在 225 °C 往复挤压 3 道次即获得了超细晶 AZ31 镁合金。随着变形温度的降低, 变形组织的平均位相差和大角度晶界的比例逐渐增加。在 3 道次的 AZ31 组织中, 只发现少量的 $\{10\bar{1}2\}$ 孪晶, 位错滑移是主要的变形机制。施密特因子计算表明, 在 225~350 °C 变形时, 锥面滑移系 $\{10\bar{1}1\}\langle 11\bar{2}0\rangle$ 被大量激活。而在 400 °C 变形时, 基面滑移系 $\{0001\}\langle 11\bar{2}0\rangle$ 被大量激活。亚晶界的详细分析为连续动态再结晶在镁合金大变形过程中晶粒细化的重要作用提供了直接的证据。

关键词: 镁合金; 晶粒细化; 连续动态再结晶; 电子背散射技术; 往复挤压

(Edited by Yun-bin HE)